

**RARE DECAYS AND EXOTIC STATES WITH BABAR**

Steven H. Robertson

*Dept. of Physics, McGill University, 3600 University St. Montreal, Quebec, Canada*  
for the *BABAR* collaboration

## Abstract

Results from the *BABAR* experiment are presented for searches for several rare FCNC *B* and *D* meson decays, including the modes  $B^0 \rightarrow \ell^+ \ell^-$  and  $D^0 \rightarrow \ell^+ \ell^-$ ,  $B \rightarrow (\rho, \omega) \gamma$  and  $B^+ \rightarrow (K, \pi)^+ \nu \bar{\nu}$ . Limits on lepton flavour violation in neutrino-less  $\tau$  decays are also discussed. Finally, results of *BABAR* searches for the strange pentaquark states  $\Theta^+(1540)$ ,  $\Xi^{--}(1860)$  and  $\Xi^0(1860)$  are summarized.

*Contributed to 19th Rencontres de Physique de la Vallée d'Aoste: Results and Perspectives in Particle Physics,*

*2/27/2005 - 3/5/2005, La Thuile, Aosta Valley, Italy*

## 1 Introduction

In addition to the CP-violation studies for which is better known, the large inclusive samples of  $B\bar{B}$ , continuum  $e^+e^- \rightarrow q\bar{q}$  and  $e^+e^- \rightarrow \tau^+\tau^-$  recorded by the *BABAR* experiment are providing unprecedented sensitivity to rare decays of heavy-flavour mesons and  $\tau$  leptons as well as to exotic states such as the controversial  $\Theta^+(1540)$  pentaquark. In these proceedings we present results of searches for a number of rare  $b \rightarrow d, s$  and  $c \rightarrow u$  flavour-changing neutral-current (FCNC) processes, the lepton-flavour violating (LFV) decay  $\tau^+ \rightarrow \mu^+\gamma$  and the strange pentaquark states  $\Theta^+(1540)$ ,  $\Xi^{--}(1860)$  and  $\Xi^0(1860)$ .<sup>1</sup>

The data used for analyses described in these proceedings were collected with the *BABAR* detector<sup>1)</sup> at the PEP-II asymmetric-energy  $e^+e^-$  storage ring at SLAC. Since 1999 the *BABAR* experiment has collected a data sample of approximately 245 million  $B\bar{B}$  pairs, corresponding to an integrated luminosity of approximately  $221 \text{ fb}^{-1}$  at the  $\Upsilon(4S)$  resonance. An additional  $23 \text{ fb}^{-1}$  sample was collected at a centre-of-mass (CM) energy approximately 40 MeV below  $B\bar{B}$  threshold and is used to study continuum production of  $e^+e^- \rightarrow q\bar{q}$  ( $q = u, d, s, c$ ) and dilepton events. *BABAR* data taking was shut down during the summer of 2004 to permit upgrades to the PEP-II accelerator and *BABAR* detector. In particular, two sextants of an upgraded muon system based on limited-streamer tubes were installed during this period. The resumption of data-taking, anticipated to begin in October 2004, was delayed by several months due to an electrical accident at SLAC, but was imminent at the time of this conference. It is anticipated that the current run will continue essentially without interruption until the summer of 2006, at which time the remaining sextants of the muon system will be installed during a several-month shutdown. It is anticipated that *BABAR* will have integrated a total luminosity of  $500 \text{ fb}^{-1}$  by the end of this run.

Charged particle tracking and  $dE/dx$  for particle identification (PID) are provided by a five-layer double-sided silicon vertex tracker and a 40-layer drift chamber contained within the magnetic field of a 1.5 T superconducting solenoid. A ring-imaging Cherenkov detector (DIRC) provides charged  $K - \pi$  separation of greater than  $3\sigma$ , over the relevant momentum range for analyses presented here. The energies of neutral particles are measured by an electromagnetic calorimeter (EMC) consisting of 6580 CsI(Tl) crystals, which provides an energy resolution of  $\sigma_E/E = (2.3/E^{1/4} \oplus 1.9)\%$  ( $E$  is in GeV). The magnetic flux return of the solenoid is instrumented with resistive plate chambers in order to provide muon identification. A full *BABAR* detector Monte Carlo (MC) simulation based on GEANT4<sup>2)</sup> is used to evaluate signal efficiencies and to identify and study background sources.

---

<sup>1</sup>Charge conjugate modes are implied throughout this paper.

## 2 $B^0 \rightarrow \ell^+\ell^-$ and $D^0 \rightarrow \ell^+\ell^-$

The leptonic decays  $B^0 \rightarrow \ell^+\ell^-$  and  $D^0 \rightarrow \ell^+\ell^-$  FCNC processes proceed via one-loop electroweak penguin and box diagrams in the Standard Model (SM). These processes are cleanly calculable, since the only non-vanishing operator is the axial-current  $O_{10}$  and the hadronic matrix elements are just the meson decay constants  $f_{B,D}$ . For  $B^0$  mesons the SM branching fractions are predicted to be  $\sim 10^{-15}$ ,  $10^{-10}$  and  $10^{-8}$  for the  $e^+e^-$ ,  $\mu^+\mu^-$  and  $\tau^+\tau^-$  modes respectively. New physics may contribute additional loop diagrams, may preferentially couple to heavier quark flavours and will not in general exhibit the helicity suppression of the SM decays. Consequently, various non-SM models predict enhancements to SM rates by two or more orders of magnitude. Experimentally,  $B^0 \rightarrow \ell^+\ell^-$  ( $\ell = e, \mu$ ) are also very clean in a B-factory environment ( $B^0 \rightarrow \tau^+\tau^-$  unfortunately is extremely challenging due to the presence of neutrinos). Results of *BABAR* searches for  $B^0 \rightarrow e^+e^-$ ,  $\mu^+\mu^-$  and the lepton-flavour violating mode  $e^+\mu^-$  based on  $111 \text{ fb}^{-1}$  of data have recently been submitted for publication<sup>3)</sup>. The experimental search proceeds by identifying two oppositely-charged high-momentum lepton candidates. The lepton four-vectors are combined to yield a  $B$  meson candidate which is expected to have invariant mass equal to the  $B$  mass and a centre-of-mass (CM) energy  $E_B$  equal to the CM beam energy  $E_{\text{beam}}$  (where the total CM energy is  $2 \cdot E_{\text{beam}}$ ). These requirements are enforced via the kinematic variables  $m_{ES} \equiv \sqrt{E_{\text{beam}}^2 - p_B^2}$  and  $\Delta E \equiv E_B - E_{\text{beam}}$ , which exploit the fact that the CM energy is very precisely determined in a B-factory environment. For  $B^0 \rightarrow \ell^+\ell^-$  the  $m_{ES}$  and  $\Delta E$  resolutions are estimated to be less than about  $3 \text{ MeV}/c^2$  and  $25 \text{ MeV}$  respectively. Additional suppression of non- $B\bar{B}$  continuum backgrounds is achieved through cuts on event-shape variables, particularly  $\cos\theta_T$ , the cosine of the angle between the thrust axis defined by the reconstructed  $B$  candidate and the thrust axis defined by the combination of all other tracks and clusters in the event. Signal efficiencies are determined from simulation, while backgrounds are determined directly from data by extrapolating  $m_{ES}$  and  $\Delta E$  sidebands into the expected signal region. Efficiency systematics arise predominantly due to knowledge of the shapes of the signal  $m_{ES}$  and  $\Delta E$  distributions, and from tracking and PID uncertainties. The total estimated systematics range from 5.7% to 7.1% for the three signal modes. Unblinding of the data revealed a total of two signal candidate in the three modes, consistent with the background expectations. Branching fraction limits are derived using a modified frequentist approach and are listed in table 1.

A related *BABAR* analysis searches for the corresponding leptonic decays of  $D^0$  mesons<sup>4)</sup>. This analysis complements the  $B^0 \rightarrow \ell^+\ell^-$  search in that it is potentially sensitive to new physics couplings of up-type quarks rather than down-type quarks.  $D^0$  candidates are reconstructed from combinations

Table 1:  $B^0 \rightarrow \ell^+ \ell^-$  results.

Mode	Efficiency	Expected background	Events observed	Limit ( 90% C.L.)
$B(B^0 \rightarrow e^+ e^-)$	$21.8 \pm 1.2$	$0.71 \pm 0.31$	0	$< 6.1 \times 10^{-8}$
$B(B^0 \rightarrow \mu^+ \mu^-)$	$15.9 \pm 1.1$	$0.72 \pm 0.26$	0	$< 8.3 \times 10^{-8}$
$B(B^0 \rightarrow e^\pm \mu^\mp)$	$18.1 \pm 1.2$	$1.29 \pm 0.44$	2	$< 18 \times 10^{-8}$

of oppositely-charged electrons and muons as described above. Due to substantial combinatorial backgrounds arising from double-semileptonic decays of  $B\bar{B}$  events, the resulting  $D^0$  candidates are required to possess CM momentum  $p_D > 2.4 \text{ GeV}/c$  and are further required to combine with a charged pion to yield a  $D^{*+} \rightarrow D^0 \pi^+$  candidate consistent with the expected  $D^{*+}$  mass. Since this analysis does not utilize  $\Upsilon(4S)$  events for the signal channel, the offpeak data is also included, for a total dataset of  $122 \text{ fb}^{-1}$ . Remaining backgrounds arise either from purely combinatorial sources or from  $D^0$  decays with kaons or pions misidentified as leptons. In the latter case, the reconstructed dilepton invariant mass is shifted slightly from the nominal  $D^0$  mass, permitting estimation of this background source directly from data sidebands along with the purely combinatorial background component. Signal yields are obtained by a simultaneous fit of the signal and background shapes to the dilepton invariant mass distribution in data, yielding branching fraction limits of

$$\begin{aligned} B(D^0 \rightarrow e^+ e^-) &< 1.2 \times 10^{-6} \\ B(D^0 \rightarrow \mu^+ \mu^-) &< 1.3 \times 10^{-6} \\ B(D^0 \rightarrow e^\pm \mu^\mp) &< 0.81 \times 10^{-6} \end{aligned}$$

at the 90% confidence level.

### 3 $B \rightarrow \rho(770)\gamma$ and $B \rightarrow \omega(782)\gamma$

Penguin-mediated  $b \rightarrow s\gamma$  FCNC decays have been relatively precisely measured in both inclusive and exclusive modes. In contrast, the CKM suppressed  $b \rightarrow d\gamma$  modes have been more elusive. The decay rates for the exclusive decays  $B \rightarrow \rho(770)\gamma$  and  $B \rightarrow \omega(782)\gamma$  are related in spectator quark models, permitting the combined rate,  $\bar{B}[B \rightarrow (\rho, \omega)\gamma]$ , to be expressed as

$$\bar{B}[B \rightarrow (\rho, \omega)\gamma] \equiv \frac{1}{2} \left\{ B(B^+ \rightarrow \rho^+ \gamma) + \frac{\tau_{B^+}}{\tau_{B^0}} [B(B^0 \rightarrow \rho^0 \gamma) + B(B^0 \rightarrow \omega \gamma)] \right\} . \quad (1)$$

The SM expectation is  $\bar{B}[B \rightarrow (\rho, \omega)\gamma] \sim (0.9-1.8) \times 10^{-6}$  but, as is the case for other FCNC decays, enhancements to this rate are predicted in various new

physics models. *BABAR* has recently reported the results of a search for the exclusive decays  $B^+ \rightarrow \rho^+\gamma$ ,  $B^0 \rightarrow \rho^0\gamma$  and  $B \rightarrow \omega(782)\gamma$  based on  $191 \text{ fb}^{-1}$  of data.  $\rho^0 \rightarrow \pi^+\pi^-$ ,  $\rho^+ \rightarrow \pi^+\pi^0$  and  $\omega \rightarrow \pi^+\pi^-\pi^0$  candidates are reconstructed from combinations of charged and neutral pions which yield invariant masses  $630 < m(\pi\pi) < 940 \text{ MeV}/c^2$  and  $764 < m(\pi^+\pi^-\pi^0) < 795 \text{ MeV}/c^2$ . These are combined with identified photons to obtain charged and neutral  $B$  meson candidates. Background arise primarily from  $e^+e^- \rightarrow q\bar{q}$  events containing energetic photons from initial state radiation,  $\pi^0/\eta$  decays, or from other radiative  $B$  decays such as  $B \rightarrow K^*\gamma$ . Events are vetoed if the photon candidate can be combined with any other photon to yield  $m(\gamma\gamma)$  consistent with a  $\pi^0$  or  $\eta$ . Additional background rejection is obtained using a combination of a neural net based on activity in the detector which is not associated with the signal photon or  $\rho/\omega$  candidate (i.e. the so-called “rest of event”), and using a Fisher discriminant based on the kinematics of the signal candidate (the helicity angle, flight direction of the reconstructed  $B$  candidate, etc.). The signal candidate yield is extracted from data using a four-dimensional extended maximum likelihood fit to the  $m_{ES}$  and  $\Delta E$  distributions and the outputs of the neural net and Fisher as shown in figure 1. Branching fraction limits are obtained both for the individual modes as well as the  $B \rightarrow (\rho,\omega)\gamma$  combination, yielding

$$\begin{aligned} B(B^+ \rightarrow \rho^+\gamma) &< 1.8 \times 10^{-6} \\ B(B^0 \rightarrow \rho^0\gamma) &< 0.4 \times 10^{-6} \\ B(B^0 \rightarrow \omega\gamma) &< 1.0 \times 10^{-6} \\ \bar{B}[B \rightarrow (\rho,\omega)\gamma] &< 1.2 \times 10^{-6} \end{aligned}$$

at 90% confidence level. These results are compared with theoretical predictions and current Belle experimental results in figure 2, from which is clear that current experimental sensitivity has reached the SM level.

Because SM  $b \rightarrow s/d\gamma$  processes are dominated by penguin diagrams with a top quark in the loop, the branching fractions are sensitive to CKM elements  $V_{tx}$  ( $x = d, s, b$ ). Although the absolute branching fractions possess relatively large theoretical uncertainties, many of these are expected to cancel in the ratio of  $b \rightarrow d\gamma$  and  $b \rightarrow s\gamma$  modes,

$$\frac{\bar{B}(B \rightarrow (\rho,\omega)\gamma)}{B(B \rightarrow K^*(892)\gamma)} = \left| \frac{V_{td}}{V_{ts}} \right|^2 \left( \frac{1 - m_\rho^2/M_B^2}{1 - m_{K^*}^2/M_B^2} \right)^3 \xi^2 [1 + \Delta R] \quad (2)$$

where  $m$  are the masses of the decay daughters,  $M_B$  is the  $B$  meson mass<sup>9)</sup>, and  $\xi$  and  $\Delta R$  are correction factors relating to flavour SU(3) breaking and weak annihilation respectively with values  $\xi^2 = 0.85 \pm 0.10$  and  $\Delta R = 0.1 \pm 0.1$ .<sup>7)</sup> Using  $\bar{B}[B \rightarrow (\rho,\omega)\gamma]$  from above and combining it with a previously published *BABAR* measurement<sup>10)</sup> of  $B(B \rightarrow K^*(892)\gamma)$  yields a limit on the

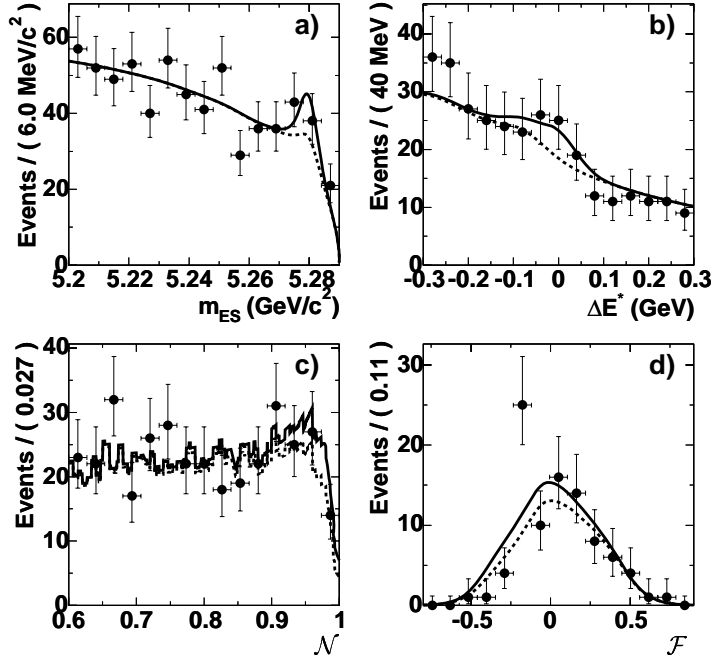


Figure 1: Projections of the combined  $B \rightarrow (\rho, \omega)\gamma$  fit to BABAR data (points) in the four fitting variables (a)  $m_{ES}$ , (b)  $\Delta E$ , (c) the neural net output  $\mathcal{N}$  and (d) the Fisher discriminant output  $\mathcal{F}$ . The dashed curves are the expected background, while the solid curves indicate the total signal plus background.

ratio  $\bar{B}(B \rightarrow (\rho, \omega)\gamma)/B(B \rightarrow K^*(892)\gamma) < 0.029$  at 90% which, neglecting theoretical uncertainties, can be interpreted as a limit on the ratio  $|V_{td}|/|V_{ts}| < 0.19$ . It is worth noting that this limit is beginning to impose a significant constraint on the  $B$  meson unitarity triangle fits.

#### 4 $B^+ \rightarrow K^+\nu\bar{\nu}$ and $B^+ \rightarrow \pi^+\nu\bar{\nu}$

The  $b \rightarrow s\nu\bar{\nu}$  branching fraction is considered to be one of the most theoretically clean probes of new physics in the  $B$  sector. Unlike the charged lepton modes  $b \rightarrow s\ell^+\ell^-$ , the neutrino modes do not possess a photonic penguin diagram (only  $Z$  penguin and  $W$  box diagrams contribute) and hence are governed by only a single Wilson coefficient.  $b \rightarrow s\nu\bar{\nu}$  is also free of long

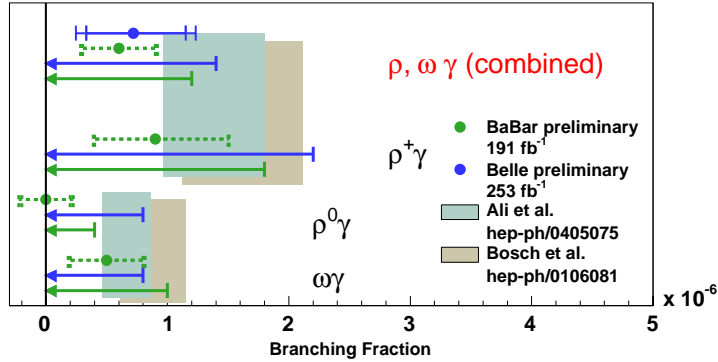


Figure 2: Comparison of  $b \rightarrow d\gamma$  branching fractions experimental results from BABAR <sup>5)</sup> and Belle <sup>6)</sup> with theoretical predictions <sup>7)</sup> <sup>8)</sup>.

distance contributions which additionally complicate the interpretation of the charged lepton modes. The situation for  $b \rightarrow d\nu\bar{\nu}$  is similar, except that there is an additional suppression factor of  $|V_{td}|^2/|V_{ts}|^2$  relative to the strange modes. Unfortunately,  $b \rightarrow s\nu\bar{\nu}$  is experimentally very difficult due to the presence of the two undetected neutrinos. Consequently, it is necessary to search for the exclusive decay  $B^+ \rightarrow K^+\nu\bar{\nu}$  rather than perform an inclusive search. The SM prediction for the  $B^+ \rightarrow K^+\nu\bar{\nu}$  branching fraction is  $\sim 4 \times 10^{-6}$ , however substantial enhancement can occur in new physics models as a result of contributions of heavy non-SM particles in the loop. BABAR has recently reported the results of a search for  $B^+ \rightarrow K^+\nu\bar{\nu}$  and  $B^+ \rightarrow \pi^+\nu\bar{\nu}$  decays based on  $82 \text{ fb}^{-1}$  of data <sup>11)</sup>. The signature for these modes is the presence of a single charged kaon or pion plus significant missing energy recoiling against a reconstructed charged  $B$  meson. The analysis proceeds by first exclusively reconstructing a charged  $B$  candidate in either an hadronic or semileptonic decay mode of the form  $B^- \rightarrow D^{(*)0} X_{\text{had}}^-$  or  $B^- \rightarrow D^{(*)0} \ell^- \bar{\nu}$ , where  $X_{\text{had}}^-$  is a combination of up to five charged or neutral hadrons. Once a charged  $B$  candidate has been identified, all remaining particles in the event are considered to comprise the signal candidate. Events are retained if the signal candidate contains exactly one track with charge opposite the reconstructed  $B$ , with CM momentum  $p_{K,\pi} > 1.25 \text{ GeV}/c$  and with PID consistent with either a kaon (for  $B^+ \rightarrow K^+\nu\bar{\nu}$ ) or pion (for  $B^+ \rightarrow \pi^+\nu\bar{\nu}$ ). True signal events may also contain a small number of low-energy calorimeter clusters resulting hadronic split-offs, beam backgrounds, bremsstrahlung photons etc., while background events typically contain significant additional calorimeter activity

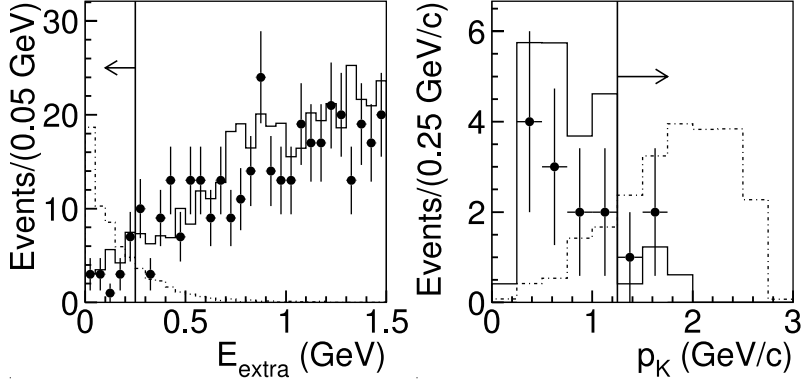


Figure 3: Distribution (a) of the total energy,  $E_{\text{extra}}$ , of all calorimeter clusters in  $B^+ \rightarrow K^+ \nu \bar{\nu}$  signal candidate events which are not used in the reconstruction of the accompanying  $B$  meson, and (b) distribution of the signal kaon CM momentum,  $p_K$  for events surviving the  $e_{\text{extra}}$  indicated in (a). Data are shown as solid points, while the MC predictions for the signal and background distributions are plotted as dashed and solid curves respectively. In both plots only events with an hadronic accompanying  $B$  are shown.

due to the presence of neutral hadrons in the event (see figure 3a). The total extra calorimeter energy associated with the signal candidate is required to be less than 250MeV. For  $B^+ \rightarrow K^+ \nu \bar{\nu}$ , the overall  $B$  reconstruction plus signal selection efficiencies were estimated to be  $(0.055 \pm 0.005)\%$  and  $(0.115 \pm 0.009)\%$  respectively for the hadronic and semileptonic reconstruction samples, dominated in both cases by the low  $B$  reconstruction efficiencies. Unblinding of the data revealed three and six events respectively, consistent with background estimates. A combined branching ratio limit of  $B(B^+ \rightarrow K^+ \nu \bar{\nu}) < 5.2 \times 10^{-5}$  is obtained using a modified frequentist approach. Comparable signal efficiencies were obtained for the  $B^+ \rightarrow \pi^+ \nu \bar{\nu}$  search, however substantially larger backgrounds were expected and subsequently observed in data, resulting in a limit of  $B(B^+ \rightarrow \pi^+ \nu \bar{\nu}) < 10 \times 10^{-5}$  at 90% confidence level.

## 5 Neutrino-less $\tau$ decays and lepton-flavour violation

In the SM with non-zero neutrino masses LFV can occur in one-loop penguin processes via neutrino mixing, but only at a level which is many orders of magnitude below current or expected future experimental sensitivity. Hence any observation of LFV would provide unambiguous evidence of new physics.



Various new physics scenarios predict enhancements in various LFV  $\tau$  decays up to the current experimental limits. *BABAR* has recently reported the results of a search for the LFV mode  $\tau^+ \rightarrow \mu^+ \gamma$ , based on a sample  $2.07 \times 10^8$   $e^+e^- \rightarrow \tau^+\tau^-$  events, corresponding to an integrated luminosity of  $232 \text{ fb}^{-1}$  (on- plus off-peak data). Events are divided into two hemispheres along a plane perpendicular to the event thrust axis and events consisting of a 1-1 or 1-3 charged track topology are retained. The so-called “tag” hemisphere is labelled as  $e$ ,  $\mu$ ,  $h$  or  $3h$  according to the particle identification of the track(s). The opposing hemisphere is then required to contain only a single muon and a photon with energy  $E_\gamma > 200 \text{ MeV}$ . Background rejection is achieved using a five-input neural net utilizing the event missing mass and transverse momentum, the tag particle momenta and the signal candidate helicity angle. Signal candidates are selected within a region defined by a  $2\sigma$  ellipse in the kinematic variables  $\delta E = E_{\mu\gamma} - \sqrt{s/2}$  and  $m_{EC}$ , defined as the invariant mass resulting from a kinematic fit to the  $\mu\gamma$  combination with  $E_{\mu\gamma}$  constrained to  $\sqrt{s/2}$ . A total of four events are observed in the combination of all tag modes. Backgrounds are determined from extrapolation of  $m_{EC}$  and  $\Delta E$  sideband regions into the signal region and are estimated to total  $6.2 \pm 0.5$  events. A branching fraction limit is derived from a maximum likelihood fit to the  $m_{EC}$  distribution (see figure 4), yielding  $B(\tau^+ \rightarrow \mu^+ \gamma) < 6.8 \times 10^{-8}$  at the 90% confidence level.

## 6 $\Theta_5^+$ (1540) and $\Xi_5^{--}$ (1860) Pentaquark searches

A flurry of recent experimental searches for pentaquark states was triggered by a theoretical paper <sup>15)</sup> based on a chiral soliton model using the  $N^+$  (1710) as input and mass splittings of  $\sim 180 \text{ MeV}c^2$ . Evidence was subsequently reported by several experimental groups for an exotic state,  $\Theta_5^+$  (1540), which is presumed to have minimal quark content of  $ududs$ . *BABAR* reported preliminary null results at ICHEP 2004 <sup>16)</sup> for the  $\Theta_5^+$  (1540),  $\Xi_5^{--}$  (1860),  $\Xi_5^0$  (1860) as well as other members of the antidecuplet and corresponding octet. These searches have recently been refined and subsequently submitted for publication <sup>17)</sup>. Since the production mechanism at an  $e^+e^-$  collider is not known the *BABAR* searches utilize all events accepted by the trigger, estimated to be more than 99% efficient for  $e^+e^- \rightarrow q\bar{q}$  events.  $\Theta^+$  candidates are reconstructed in the mode  $pK_s^0$  ( $K_s^0 \rightarrow \pi^+\pi^-$ ), with a resulting invariant mass resolution ranging from 2-8  $\text{MeV}/c$  depending on the signal candidate momentum. The signal efficiency is estimated from Monte Carlo simulation and validated by comparing the data yield for  $\Lambda_c^+ \rightarrow pK_s^0$  with the simulation predictions. A clear  $\Lambda_c^+ \rightarrow pK_s^0$  peak containing approximately 98000 events is visible in data, however no evidence of the  $\Theta_5^+$  (1540) is visible (see figure 5 left). Limits are obtained by fitting both the inclusive  $pK_s^0$  spectrum and the differential spectra obtained in

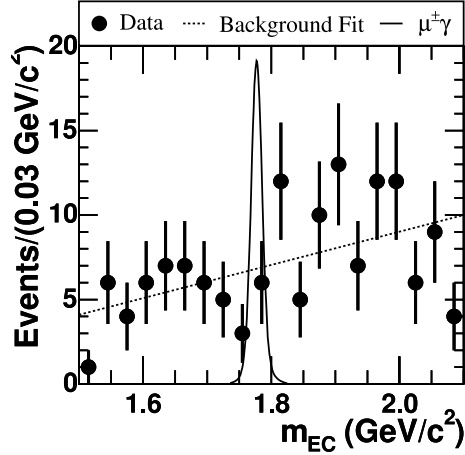


Figure 4: *The energy-constrained invariant mass  $m_{EC}$  for  $\tau^+ \rightarrow \mu^+ \gamma$  signal candidate events. Data are shown as solid points, while the fitted background shape is shown as a dashed curve. The signal shape is shown for illustration as a solid curve.*

bins of the CM  $pK_s^0$  candidate momenta (figure 5 right and table 2) assuming both a width of  $1 \text{ MeV}/c^2$  and a natural width of  $8 \text{ MeV}/c^2$ . Production rates are consistent with zero across the entire momentum range and for all width hypotheses.

Searches for the  $\Xi_5^{--}(1860)$  and  $\Xi_5^0(1860)$  pentaquarks proceed in a similar manner, via the channels  $\Xi_5^{--}(1860) \rightarrow \Xi^- \pi^-$  and  $\Xi_5^0(1860) \rightarrow \Xi^- \pi^+$ , where  $\Xi^- \rightarrow \Lambda^0 \pi^-$ ,  $\Lambda^0 \rightarrow p \pi^-$ . A total of 290000  $\Xi^-$  candidates are obtained, with a signal to background ratio of 23:1 in the  $\Lambda^0 \pi^-$  invariant mass. The overall reconstruction efficiency for  $\Xi_5^{--}(1860)$  and  $\Xi_5^0(1860)$  is estimated to range from 6.5% at low momentum to 12% at high momentum. The  $\Xi_5^0(1860)$  efficiency is further validated by comparing the yield of conventional  $\Xi^0(1530)$  and  $\Xi_c$  baryons in data and simulation. Signal yields are extracted both inclusively and in bins of momentum as was done in the  $\Theta^+$  search, for signal widths ranging from 1-18  $\text{MeV}/c^2$ . No evidence for either  $\Xi_5^{--}(1860)$  or  $\Xi_5^0(1860)$  was found. The resulting limits are reported in table 2.

## 7 Summary

We have reported the results of *BABAR* searches for several rare decays with potential sensitivity to beyond-SM physics. In several cases, such as  $B \rightarrow (\rho, \omega) \gamma$

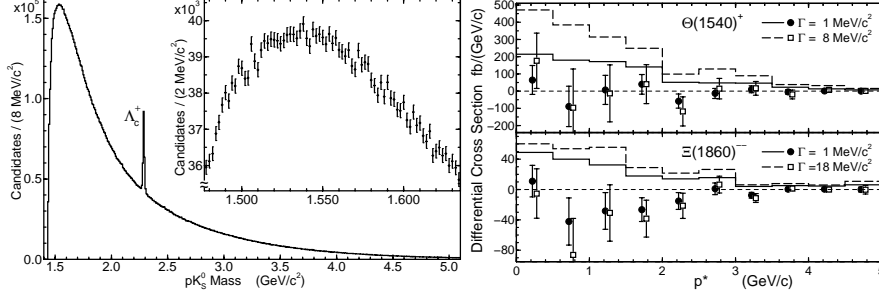


Figure 5: The  $pK_s^0$  invariant mass distribution (left), with detail of the  $\Theta_5^+(1540)$  signal region shown inset. Limits on the differential production cross section (right) for  $\Theta_5^+(1540)$  and  $\Xi_5^{--}(1860)$  in bins of the signal candidate CM momentum assuming two different possible decay widths (solid and dashed lines).

Table 2: Pentaquark search results integrated over the entire momentum range and quoted as both cross section upper limits and in terms of the rate per event. Numbers in brackets assume ( $\Lambda =$  natural width), while unbracketed numbers assume ( $\Lambda = 1 \text{ MeV}/c^2$ ).

Pentaquark state	Cross section upper limit (fb)	$e^+e^- \rightarrow q\bar{q}$ yield upper limit ( $\times 10^5/\text{event}$ )
$\Theta^+ + \Theta^-$	171 (363)	5 (11)
$\Xi_5^{--} + \Xi_5^{++}$	25 (36)	0.74 (1.1)

and  $B^+ \rightarrow K^+ \nu \bar{\nu}$ , these limits are approaching SM predictions. In other cases, such as  $B^0 \rightarrow \ell^+ \ell^-$  and  $\tau^+ \rightarrow \mu^+ \gamma$ , the current experimental limits are many orders of magnitude from the SM, but the limits are currently constraining new physics. In addition, we have described searches for the strange pentaquark states  $\Theta_5^+(1540)$ ,  $\Xi_5^{--}(1860)$  and  $\Xi_5^0(1860)$ . While large, cleanly reconstructed samples of similar conventional baryons are obtained with excellent invariant mass resolution, we see no evidence of these pentaquark states and conclude that if they exist, then production must be significantly suppressed in  $e^+e^-$  compared to conventional baryons.

## References

1. B. Aubert *et al.*(*BABAR* Collaboration), Nucl. Instrum. Meth. **A479**, 1 (2002).
2. S. Agostinelli *et al.*, [GEANT4 Collaboration], Nucl. Inst. Meth. **A506**, 250 (2003).
3. B. Aubert *et al.*(*BABAR* Collaboration), hep-ex/0408096 (Aug 2004) 7p. (submitted to Phys. Rev. Lett.).
4. B. Aubert *et al.*(*BABAR* Collaboration), Phys. Rev. Lett. **93**, 191801 (2004).
5. B. Aubert *et al.*(*BABAR* Collaboration), Phys. Rev. Lett. **94**, 011801 (2005).
6. K. Abe *et al.*(Belle Collaboration), hep-ex/0408137 (Aug 2004) 10p..
7. A. Ali, E. Lunghi, A. Y. Parkhomenko, Phys. Lett. B **595**, 323, (2004); hep-ph/0405075.
8. S. Bosch and G. Buchalla, Nucl. Phys. **B621** 459-478 (2002); hep-ph0106081.
9. Particle Data Group, S. Eidelman *et al.*, Phys. Lett. B **592**, 1 (2004).
10. B. Aubert *et al.*(*BABAR* Collaboration), Phys. Rev. D **70**, 112006 (2004).
11. B. Aubert *et al.*(*BABAR* Collaboration), Phys. Rev. Lett. **94**, 101801 (2005).
12. B. Aubert *et al.*(*BABAR* Collaboration), hep-ex/0502032 (Feb 2005) 7p. (submitted to Phys. Rev. Lett.).
13. B. Aubert *et al.*(*BABAR* Collaboration), Phys. Rev. Lett. **92**, 121801 (2004).
14. B. Aubert *et al.*(*BABAR* Collaboration), hep-ex/0409036 (Sep 2004) 17p.
15. D. Diakonok, V. Petrov and M. Polyakov, Z. Phys. **A 359**, 305 (1997).
16. B. Aubert *et al.*(*BABAR* Collaboration), hep-ex/0408064 (Aug 2004) 22p..
17. B. Aubert *et al.*(*BABAR* Collaboration), hep-ex/0502004 (Feb 2005) 7p. (submitted to Phys. Rev. Lett.).